

Effects on the physical properties of cation substitution in the layered cobaltites $Y(\text{Ba}_{1-x}\text{Ca}_x)\text{Co}_2\text{O}_{5.5}$

G. Aurelio^{a,*}, J. Curiale^a, R.D. Sánchez^a, G.J. Cuello^b

^aCNEA—Centro Atómico Bariloche, Bustillo 9500, 8400, S.C. de Bariloche, Río Negro, Argentina

^bInstitut Laue Langevin, BP 156, F-38042 Grenoble Cedex 9, France

Abstract

In this work we study the physical properties of the layered cobaltites $Y\text{BaCo}_2\text{O}_{5.5}$, focussing on the role of cationic disorder and size effects by a partial substitution of Ba by Ca. We have synthesized the polycrystalline compounds $Y(\text{Ba}_{1-x}\text{Ca}_x)\text{Co}_2\text{O}_{5.5}$ with $x = 0, 0.05$ and 0.10 . We characterized the samples within the 5–500 K temperature range, using neutron diffraction, magnetic measurements and electrical resistivity experiments. We have found the magnetic properties to be strongly affected by the cationic substitution. Although the “122” perovskite structure seems unaffected by Ca addition, the magnetic arrangements of Co ions are drastically modified: the antiferromagnetic (AFM) long-range order is destroyed, and a ferrimagnetic phase is stabilized below $T \sim 290$ K. For the sample with $x = 0.05$ a small fraction of AFM phase seems to coexist with a ferrimagnetic one below $T \sim 190$ K, whereas for $x = 0.10$ the AFM order is completely lost.

© 2007 Elsevier B.V. All rights reserved.

PACS: 75.30.Kz; 75.47.Pq; 72.20.Pa; 61.50.Nw

Keywords: Magnetic oxides; Cobalt perovskites; Magnetic susceptibility; Neutron diffraction; Electrical resistivity

1. Introduction

The oxygen-deficient layered perovskites $\text{R}\text{BaCo}_2\text{O}_{5+\delta}$ (where R is a rare earth element) show very interesting and extremely rich physical properties. These compounds are oxygen non-stoichiometric ($0 \leq \delta < 1$) which allows the 3d cobalt cation to adopt different oxidation states. The compounds in which Co ions have an average 3+ valence ($\delta = 0.5$) are particularly interesting because at this composition a structural arrangement of oxygen leads to the ordering of Co ions in two crystallographic sites corresponding to pyramidal and octahedral oxygen coordinations, the so-called “122” superstructure. Moreover, the spin state of each Co atom is dependent on such oxygen coordination and can take the values $S = 0, 1$ and 2 , which is an issue of intense debate in the literature.

Among the cobalt oxides synthesized in the last years, the compound with $\text{R} = \text{Y}^{3+}$, which is a small, non-magnetic ion, is a good candidate to isolate the intrinsic properties of Co in the layered perovskite. In this work, we study the structural, magnetic and transport properties of cobaltites with $\text{R} = \text{Y}^{3+}$, focussing on the role of cationic disorder and size effects by substituting the Ba-site with Ca, which has a smaller atomic radius and is therefore expected to introduce a certain degree of distortion and disorder. The objective of the present work is to characterize and correlate the various physical properties in the substituted compounds when compared to the parent $Y\text{BaCo}_2\text{O}_{5.5}$ cobaltite.

Polycrystalline samples of $Y(\text{Ba}_{1-x}\text{Ca}_x)\text{Co}_2\text{O}_{5.5}$ with $x = 0, 0.05$ and 0.10 were prepared by solid-state reaction, as explained in a previous work [1]. A new, single batch was prepared with all the samples to guarantee identical synthesis conditions. We have not explicitly determined the oxygen content in the samples, but our structural data are in excellent agreement with published data [2], indicating that the parent sample contains $\delta \approx 0.50$.

*Corresponding author.

E-mail address: gaurelio@cab.cnea.gov.ar (G. Aurelio).

2. Results

We have shown in a previous study [1] that the magnetization of the parent compound $\text{YBaCo}_2\text{O}_{5.5}$ presents two characteristic temperatures: T_C corresponding to a sudden increase of the magnetization very close to room temperature, and T^* at which the magnetization abruptly drops to zero. The main magnetic interactions at low temperature between the Co spins were found to be antiferromagnetic (AFM), indicating that at T^* a transition to an AFM state occurs [1]. In the present work, not only we extend our previous study by replacing 5% and 10% of Ba ions with smaller Ca cations, but we also make use of the neutron diffraction technique to gain insight into the different magnetic arrangements of the Co ions. In Fig. 1 we show the low-field magnetization measurements as a function of temperature for samples $\text{Y}(\text{Ba}_{1-x}\text{Ca}_x)\text{Co}_2\text{O}_{5.5}$ with $x = 0, 0.05$ and 0.10 . The magnetic moment as a function of temperature was obtained using a MPMS quantum design SQUID. Empty symbols represent the FCC magnetization measured on cooling from 310 to 5 K under a magnetic field of 5 kOe, and solid symbols represent the magnetization subsequently measured on warming (FCW). The estimated T_C temperatures are ≈ 287 K for the three studied samples, indicating that the transition at T_C is unaffected by Ca substitution. On the other hand, the magnetization at low temperatures is drastically increased by the addition of Ca, showing a destabilization of the AFM phase. An interesting feature to remark is the important degree of thermal hysteresis, particularly in the $x = 0.05$ sample. It is also worth noticing that the $x = 0$ sample corresponds to a different batch than the one previously reported [1] but nevertheless shows an identical behavior. However, the T_C

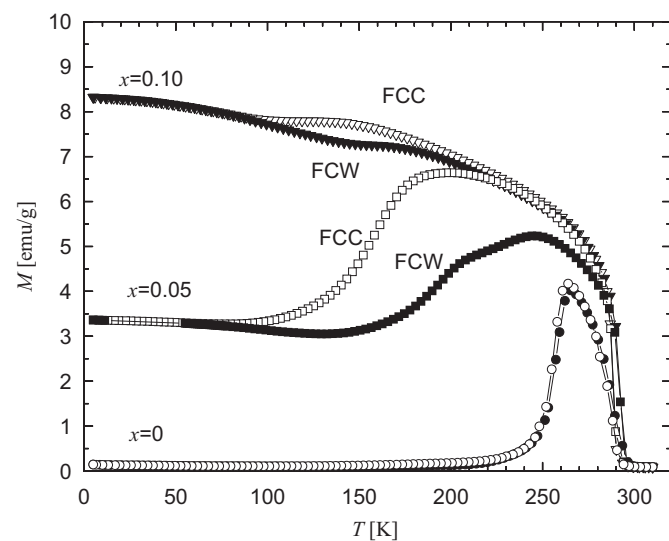


Fig. 1. Low-field magnetization as a function of temperature for samples with $x = 0, 0.05$ and 0.10 . Empty symbols represent the FCC magnetization measured on cooling under a magnetic field of 5 kOe, and solid symbols represent the magnetization subsequently measured on warming (FCW).

is somewhat lower in the present case, probably due to a slight difference in the oxygen content, which indicates that oxygen plays a more fundamental role in this transition than Ca doping.

Fig. 2 shows the temperature dependence of the inverse susceptibility of samples with $x = 0$ (upper panel) and $x = 0.10$ (lower panel) in the temperature range $250 \text{ K} \leq T \leq 473 \text{ K}$. The experiments were performed on a home-made Faraday balance under a 5 kOe field, at a warming/cooling rate of 0.7 K/min in a 1 Torr air atmosphere. The maximum temperature of 473 K was selected to ensure that no oxygen loss occurred in the samples, according to our previous results [1]. Following a simple Curie–Weiss model, the high-temperature data extrapolate linearly to $\theta \approx -75 \text{ K}$ and $\theta \approx 110 \text{ K}$ for $x = 0$ and $x = 0.10$, respectively, as indicated by the arrows. This means that the cation replacement by Ca reverts the sign of θ , showing that AFM interactions get weaker when cation disorder is greater. The abrupt drop in the inverse of susceptibility when the temperature approaches T_C on cooling can be very well accounted for by a simple phenomenological model for ferrimagnets [3]. The idea that these compounds

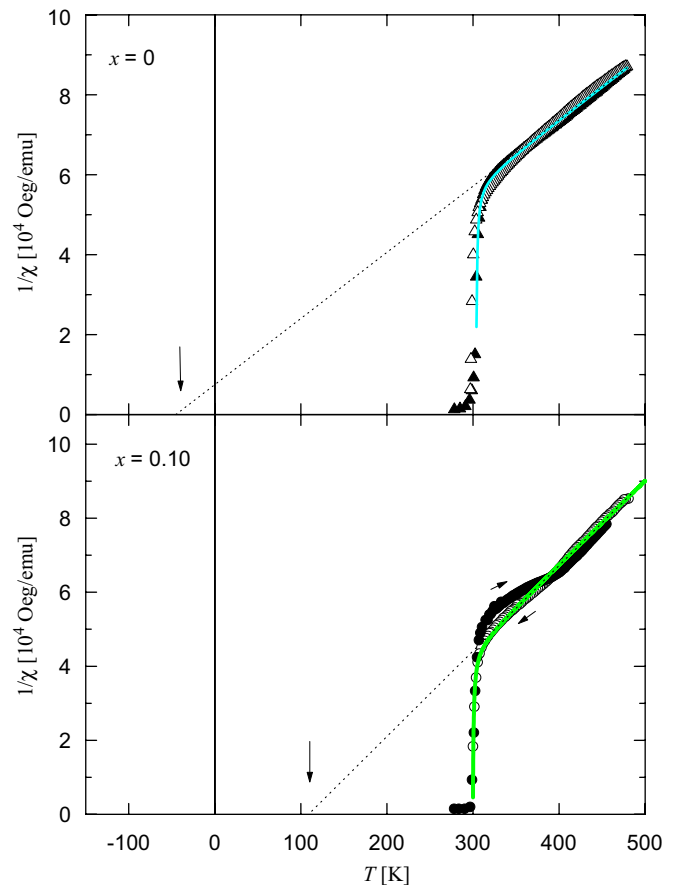


Fig. 2. Temperature variation of the inverse susceptibility of $\text{Y}(\text{Ba}_{1-x}\text{Ca}_x)\text{Co}_2\text{O}_{5.5}$ for samples with $x = 0$ and 0.10 . Open symbols and solid symbols correspond to data collected on cooling and warming, respectively. The dashed lines are only a guide to the eye. The solid lines represent a fit to the data using a phenomenological model for ferrimagnets [3].

behave as ferrimagnets in a given temperature range has already been proposed in previous works [4–6], in which Co atoms at different crystallographic sites are in different spin states. As we shall see, our neutron diffraction data give further support to this hypothesis.

Electrical resistivity measurements were performed under zero-applied magnetic field and under a 90 kOe applied field, using the standard four-probe technique with gold contacts sputtered onto the samples to reduce contact resistance. The zero-field electrical resistivity of samples $x = 0$ and 0.10 is shown in Fig. 3 for the temperature range $80 \text{ K} < T < 300 \text{ K}$. The electrical resistivity of both samples shows a sharp step corresponding to the metal–insulator transition; for the $x = 0$ compound the transition lies approximately at room temperature, while in the Ca-substituted sample $x = 0.10$ it lies at 290 K. For a field of 90 kOe we did not observe any significant difference with the zero-field resistivity measurements.

Neutron powder diffraction (NPD) data were collected on the high-intensity two-axis diffractometer D20 located at the High Flux Reactor of Institute Laue-Langevin ILL, Grenoble, France. Samples with $x = 0.05$ and 0.10 were cooled in a standard orange cryostat from room temperature down to 20 K, and diffraction patterns were then collected every two minutes at a warming rate of 1 K/min up to 320 K. A wavelength of $\sim 2.41 \text{ \AA}$ was used to highlight the magnetic diffraction. In addition, high-resolution NPD data were collected at diffractometer D2B of ILL for samples with $x = 0, 0.05$ and 0.10, using a wavelength of $\sim 1.594 \text{ \AA}$ to collect patterns at selected temperatures. The processing of the NPD patterns with the full-pattern analysis Rietveld method, is still under way and will be published elsewhere. The room temperature structure of $\text{RBaCo}_2\text{O}_{5+\delta}$ has been described in detail in various references [1,7]. For $\delta = 0.5$ it corresponds to the $Pnmm$ orthorhombic space group with a unit cell $a_P \times 2a_P \times 2a_P$ (“122”).

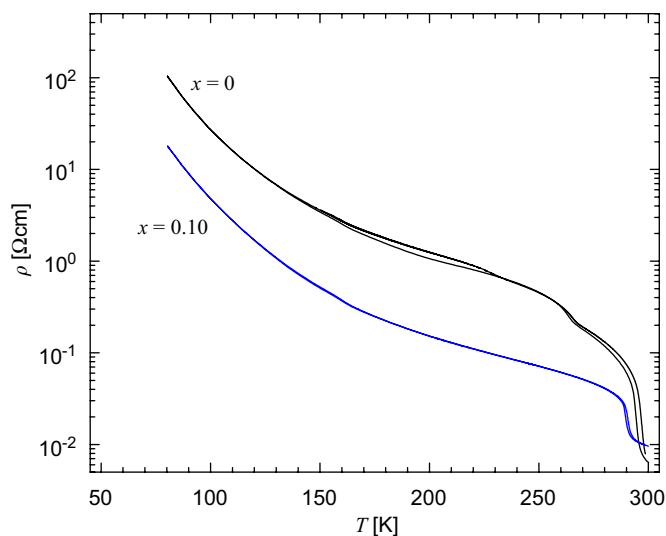


Fig. 3. Resistivity curves for $\text{Y}(\text{Ba}_{1-x}\text{Ca}_x)\text{Co}_2\text{O}_{5.5}$ for samples with $x = 0$ and 0.10 collected on cooling and warming in the range $80 \text{ K} < T < 300 \text{ K}$.

In Fig. 4 we show a selected area ($70^\circ < 2\theta < 85^\circ$) of the thermodiffractograms corresponding to samples with $x = 0.05$ (a) and $x = 0.10$ (b). The evolution with temperature (y -axes) of the (040) and (200) Bragg reflections of the “122” phase, clearly shows the existence of structural changes accompanying the magnetic and electronic transitions presented in the previous sections. The insets in Fig. 4(a) and (b) correspond to a 2D projection of the thermodiffractograms in the selected range. For the sample with $x = 0.05$, two major changes are indicated by arrows: the first one occurs at $T \approx 290 \text{ K}$ and corresponds to a sudden distortion of the orthorhombic “122” nuclear phase, in which the unit cell expands in the b -axis direction and shrinks in the a -axis direction. This distortion has been shown to be concomitant with the metal–insulator transition in related cobaltites [8] and has been associated to an orbital ordering due to the electron delocalization in high-spin Co^{3+} ions taking place at T_{MI} . The same effect is observed in the $x = 0.10$ sample, at $T \approx 293 \text{ K}$. At the same time, some reflections disappear in both diffraction patterns, as shown in Fig. 5(a) and (b) corresponding to a 2D projection in the low 2θ region. These reflections, of magnetic nature, correspond to a magnetic cell which is doubled in the a -axis direction (propagation vector $(\frac{1}{2}00)$). A more detailed analysis of the magnetic structures is still under way, but there seems to be a good agreement with the ferrimagnetic model proposed by Plakhty et al. [9] and Khalyavin [6]. Moreover, the sample with $x = 0.05$ shows an extra set of reflections which disappear at $T \approx 190 \text{ K}$ on warming. One of these reflections is clearly observed in Fig. 4(a) and its inset, as a new peak growing between the two nuclear ones. Fig. 5(a) shows, too, that there are other peaks at lower angles which, although weak, are clearly arising at $T \approx 190 \text{ K}$. To understand this set of reflections, it is useful to examine the high resolution data. In Fig. 5(c) we present the low-angle region of the NPD patterns from D2B ($\lambda \approx 1.594 \text{ \AA}$) for samples with $x = 0, 0.05$ and 0.10 collected for 4 h at 70 K. Three sets of vertical bars are shown at the bottom, representing the Bragg reflections for the nuclear “122” phase (bottom set), a magnetic cell “222” with a propagation vector $(\frac{1}{2}00)$ and a magnetic cell “224” with a propagation vector $(\frac{1}{2}0\frac{1}{2})$. The asterisks in the $x = 0$ pattern indicate those reflections which could be accounted for with this latter magnetic cell, and represent the AFM phase characteristic of the parent compound $\text{YBaCo}_2\text{O}_{5.5}$. These reflections are those which seem to be also present in the $x = 0.05$ sample according to Fig. 5(a), although with weaker intensities what means that there is a smaller amount of this phase in the latter sample, coexisting with the “222” magnetic phase.

3. Summary and remarks

We have successfully synthesized the doped layered cobaltites $\text{Y}(\text{Ba}_{1-x}\text{Ca}_x)\text{Co}_2\text{O}_{5.5}$ for $x = 0, 0.05$ and 0.10. We have found that the alkaline earth doping strongly

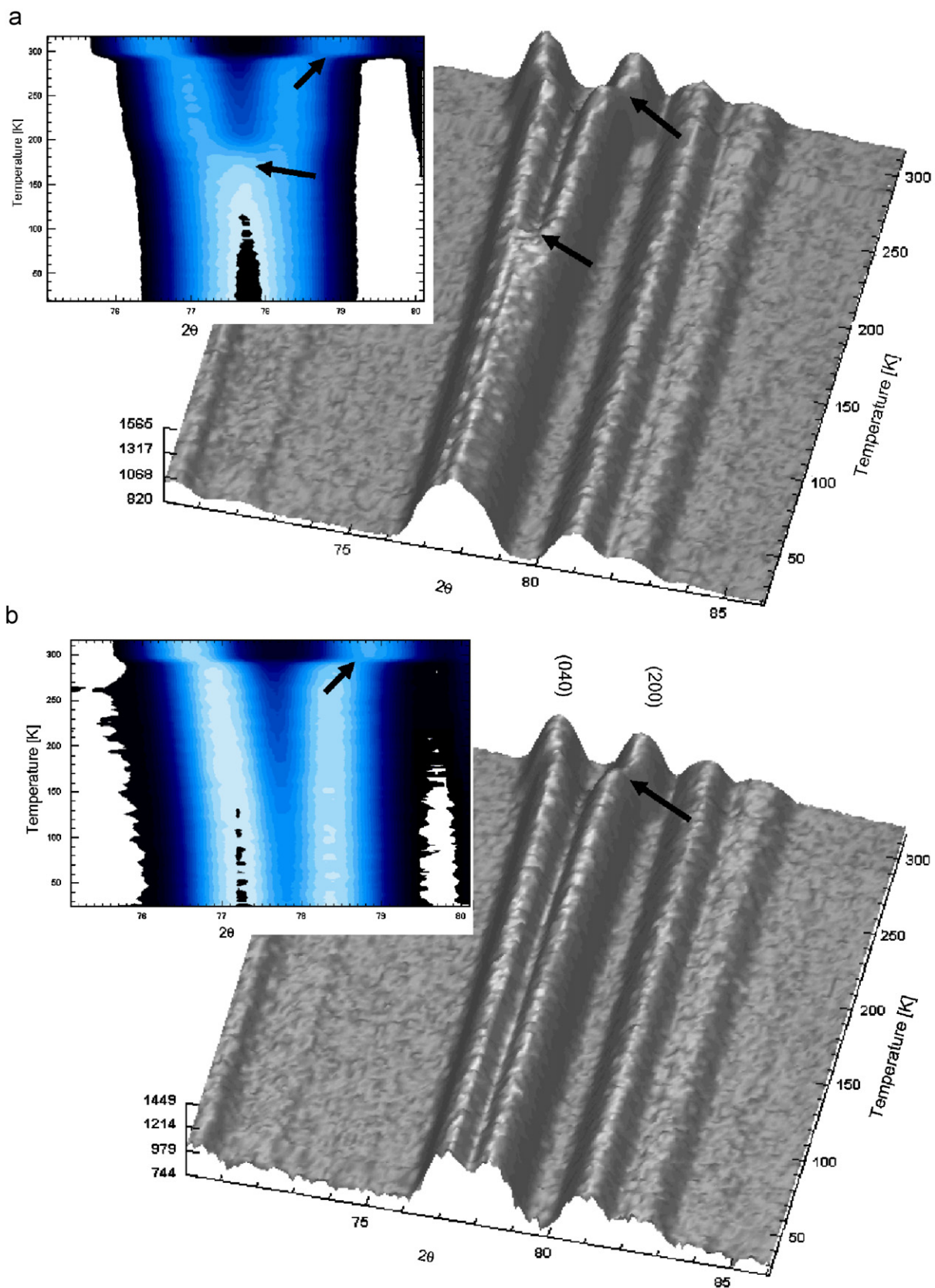


Fig. 4. Selected area of the thermodiffractograms corresponding to samples with $x = 0.05$ (a) and $x = 0.1$ (b). Collected at D20 with $\lambda \approx 2.41 \text{ \AA}$ between 20 and 320 K. The insets correspond to a 2D projection of the same 2θ region. The arrows indicate the temperatures at which the diffraction patterns show major changes during the temperature scans.

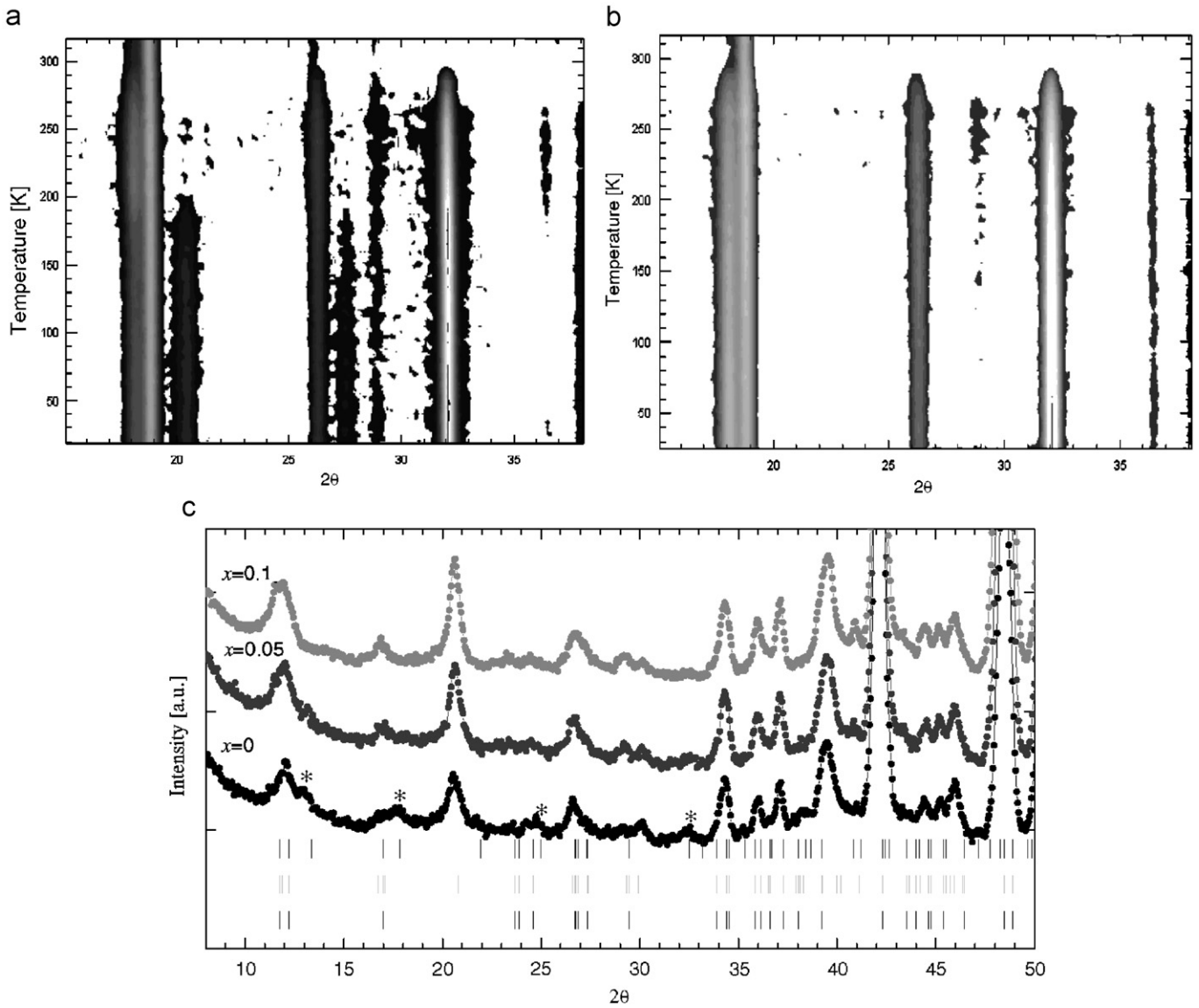


Fig. 5. 2D projection of the thermodiffractograms in the low diffraction angle region for samples $x = 0.05$ (a) and $x = 0.10$ (b). Data collected at D20 with $\lambda \approx 2.41 \text{ \AA}$ between 20 and 320 K. (c) Low-angle region of the NPD patterns at D2B ($\lambda \approx 1.594 \text{ \AA}$) for samples with $x = 0, 0.05$ and 0.10 at 70 K. The sets of vertical bars at the bottom are described in the text.

affects the magnetic properties of the parent compound $\text{YBaCo}_2\text{O}_{5.5}$. With the partial substitution of Ba with smaller cations as Ca, we could highlight the competition between the AFM orders observed in various $\text{RBaCo}_2\text{O}_{5.5}$ cobaltites, and the ferrimagnetic phase which is generally observed in a narrow temperature range. For the sample with $x = 0.05$ a small fraction of AFM phase seems to coexist with a ferrimagnetic one below $T \sim 190 \text{ K}$, whereas for $x = 0.10$ the AFM order is completely lost. Although our NPD analysis is in a preliminary stage, our findings give support to the complex scenario proposed in recent works [9,6,10]. The structural distortion observed in our NPD is probably associated to the metal-insulator rather than to the paramagnetic to ferrimagnetic transition. Unfortunately, both phenomena are almost coincident in

the compound with $\text{R} = \text{Y}$. Recent studies in other members of the cobaltites family indicate that the distortion is associated to a charge delocalization [8] rather than a spin-state transition as proposed previously [4]. In fact, our high-temperature susceptibility data do not agree either with the mentioned spin transition.

Acknowledgments

G.A. and R.D.S. are members of CONICET. This work was financed by the following projects: U.N. Cuyo 06/C203; ANPCyT PICT-2004 21372; PIP-CONICET 5250. We thank ILL for the beamtime allocation and its staff for their kind help and technical assistance.

References

- [1] G. Aurelio, J. Curiale, R.D. Sánchez, R.E. Carbonio, *Physica B* 384 (2006) 106.
- [2] D. Akahoshi, Y. Ueda, *J. Phys. Soc. Japan* 68 (1999) 736; D. Akahoshi, Y. Ueda, *J. Solid State Chem.* 156 (2001) 355.
- [3] J.S. Smart, *Effective Field Theories of Magnetism*, Saunders, London, 1966 (Chapter 12).
- [4] C. Frontera, J.L. García-Muñoz, A. Llobet, M.A.G. Aranda, *Phys. Rev. B* 65 (2002) 180405(R).
- [5] A.A. Taskin, A.N. Lavrov, Y. Ando, *Phys. Rev. Lett.* 90 (2003) 227201.
- [6] D.D. Khalyavin, *Phys. Rev. B* 72 (2005) 134408.
- [7] M. Respaud, C. Frontera, J.L. García-Muñoz, M.A.G. Aranda, B. Raquet, J.M. Broto, H. Rakoto, M. Goiran, A. Llobet, J. Rodríguez-Carvajal, *Phys. Rev. B* 64 (2001) 214401.
- [8] E. Pomjakushina, K. Conder, V. Pomjakushin, *Phys. Rev. B* 73 (2006) 113105.
- [9] V.P. Plakhty, Yu.P. Chernenkov, S.N. Barito, A. Podlesnyak, E. Pomjakushina, E.V. Moskvina, S.V. Gavrilov, *Phys. Rev. B* 71 (2005) 214407.
- [10] B. Raveau, Ch. Simon, V. Caignaert, V. Pralong, F.X. Lefevre, *J. Phys.: Condens. Matter* 18 (2006) 10237.